Supporting Information

Exploring Electronic and Excitonic Processes Towards Efficient Deep Red $CuInS_2$/ZnS Quantum-dot Light-emitting Diodes

Ting Wang, Xin Guan, Hanzhuang Zhang,* and Wenyu Ji*

Key Lab of Physics and Technology for Advanced Batteries (*Ministry of Education*), *College of Physics, Jilin University, Changchun, 130023, China*

*zhanghz@jlu.edu.cn; jiwy@jlu.edu.cn;

The QDs possess an average diameter of 4.2 nm, characterized by a PL emission peak at 627 nm in ethanol (Figure S1). Compared with the PL in ethanol, the emission of QD film shows a redshift, from 627 to 650 nm as shown in Figure S1b, which is partly attributed to the energy transfer from the QDs with high exciton energy to the ones with low exciton energy. In addition, $CuInS_2$/ZnS QDs display a large Stokes shift and a highly broad PL emission with the full width at half maximum (FWHM) of approximate 120 nm due to the nonexcitonic and surface defects associated optical properties in the multinary QDs.[1-2]

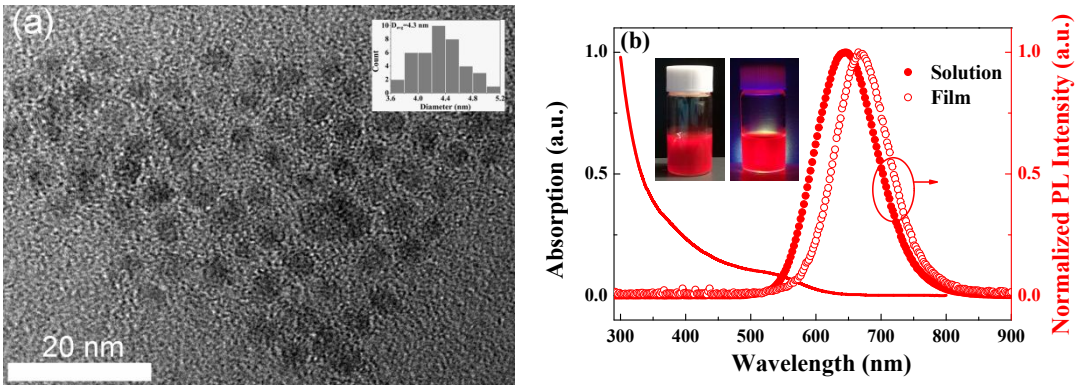

Figure S1 (a) TEM images of $CuInS_2$/ZnS QDs. Inset is the size distribution histogram and the diameter of QD was ~4.3 nm. (b) PL and absorption spectra of QDs in ethanol, as well as the PL spectrum of QDs on glass. Inset is the fluorescent photograph of QDs in toluene.

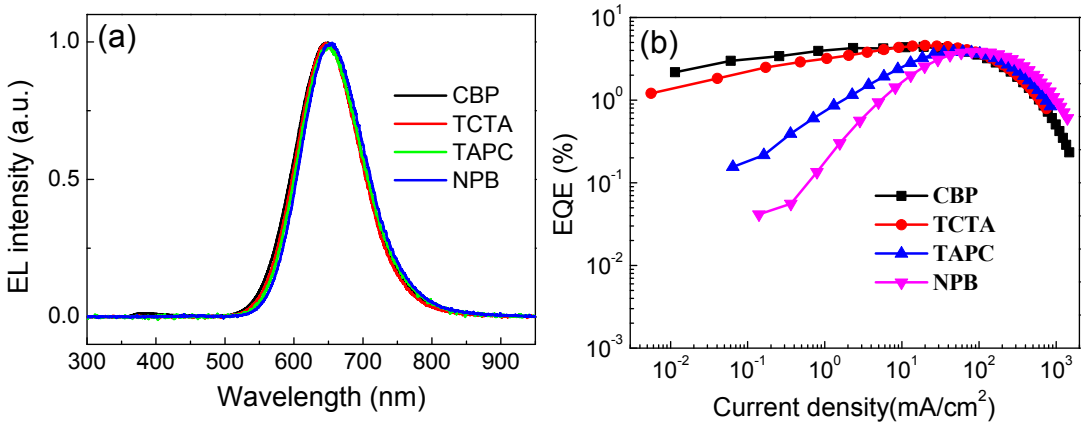

Figure S2 (a) EL spectra and (b) EQE versus driving current properties of the QLEDs based on different HTLs.

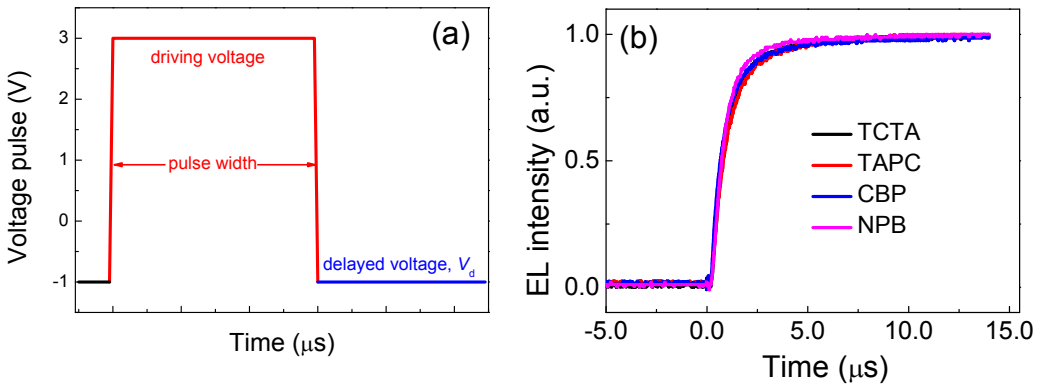

Figure S3 (a) Voltage pulse used in this work to drive the devices, (b) the rising edges of the TREL spectra for different devices. The delayed times are nearly identical for these four devices.

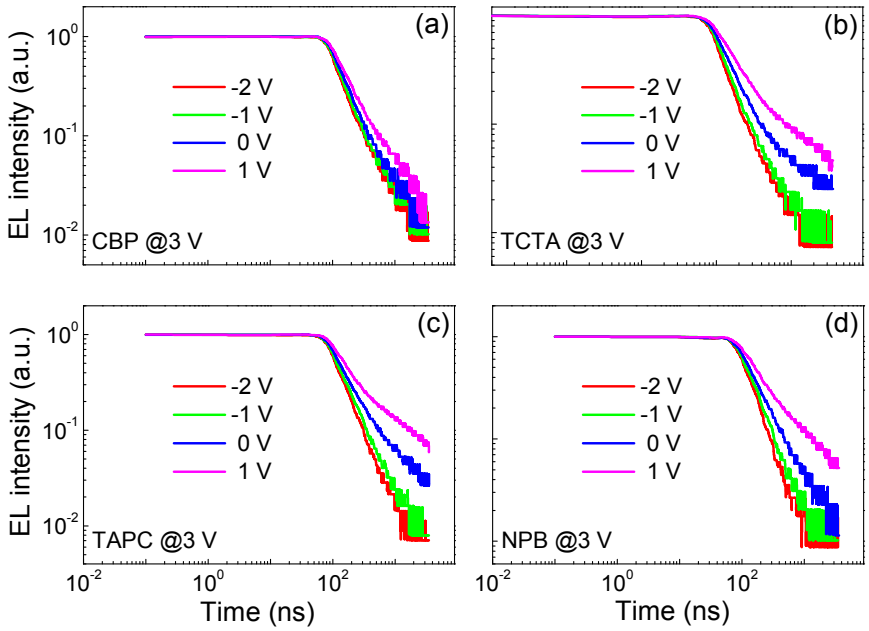

Figure S4 Normalized intensity of transient EL (the falling edge under different delayed voltages V_d) of devices with different HTLs, (a) CBP, (b) TCTA, (c) TAPC, and (d) NPB.

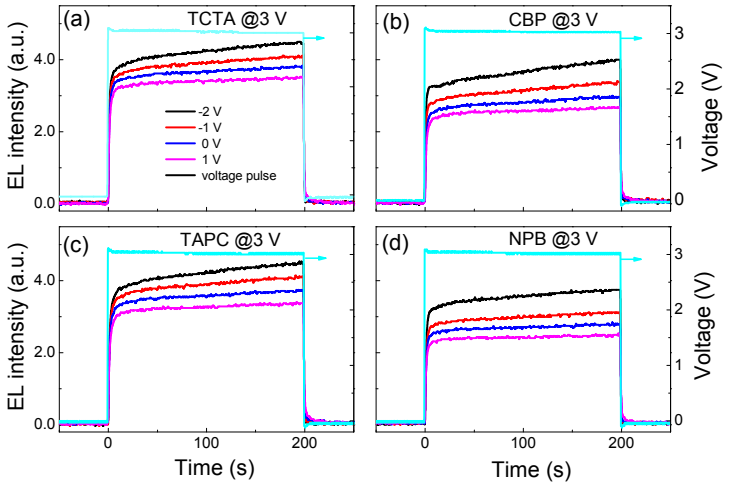

Figure S5 Intensity of whole transient EL spectra of different devices driven by a 3 V pulse voltage, (a) CBP, (b) TCTA, (c) TAPC, and (d) NPB.

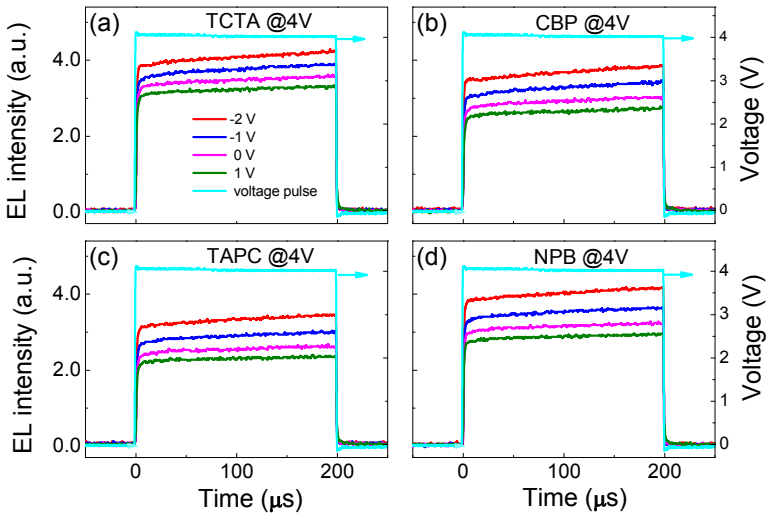

Figure S6 Intensity of whole transient EL spectra of different devices, driven by a 4 V pulse voltage, (a) CBP, (b) TCTA, (c) TAPC, and (d) NPB.

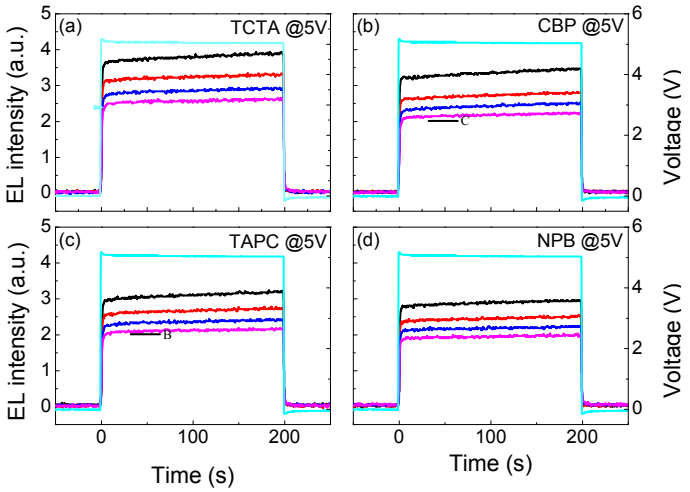

Figure S7 Intensity of whole transient EL spectra of different devices driven by a 5 V pulse voltage, (a) CBP, (b) TCTA, (c) TAPC, and (d) NPB.

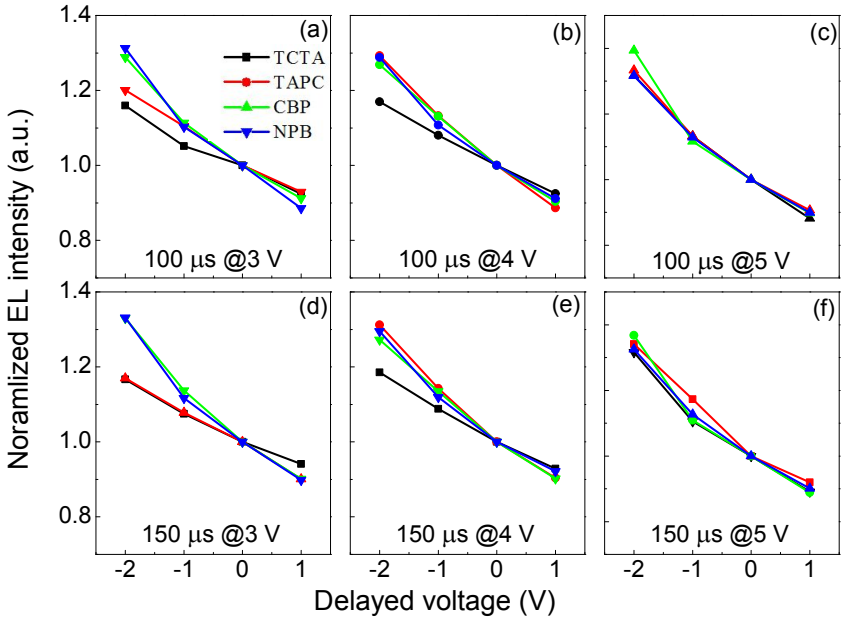

Figure S8 Normalized EL intensity of devices as a function of the delayed voltage V_d, (a) 3 V, (b) 4 V, and (c) 5 V at 100 μs; (d) 3 V, (e) 4 V, and (f) 5 V at 150 μs.

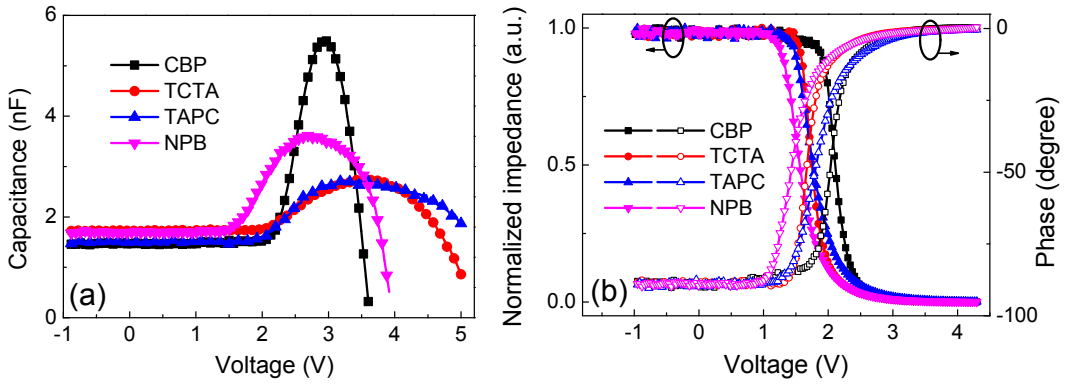

Figure S9 (a) Capacitance-voltage and (b) impedance-voltage-phase properties of QLEDs with different HTLs.

To further evaluate the carrier distribution and recombination zone in the devices, we implement the capacitance measurements and the results are shown in Figure S9a. The ascent of the capacitance indicates that the carrier begins to accumulate at a certain interface and the corresponding layer is approaching the flat-band conditions.[3] It has been demonstrated that the flat-band conditions were always satisfied for the ZnO electron transport layer due to its high conductivity.[4] As a result, the rise of the capacitance should be due to the injection of holes from Al/MoO_3 anode, leading to the increase of the HTL conductivity. Simultaneously, the injected holes will form excitons with the accumulated electrons at QDs/HTL interface, generating EL emission. This is the case for the devices with CBP, TCTA, and TAPC as the HTLs, in which the voltages for the capacitance raising are identical to the EL turn-on voltages as observed from Figure 2b in the main text. However, the NPB based device shows an abnormal phenomenon that the capacitance begins to ascend at a voltage much lower than the EL turn-on voltage. This can be attributed to the electron leakage from QDs to NPB due to the high electron mobility. Figure S9b is the impedance–voltage–current phase curves of QLEDs with different HTLs. The voltage

values, at which the impedance abruptly decreases, are identical to that for the sharp rise of the current phase. Similarly, the ascent of the current phase for the NPB based device under low applied voltages should not originate from the carrier recombination, but from the electron leakage from QDs into the NPB.

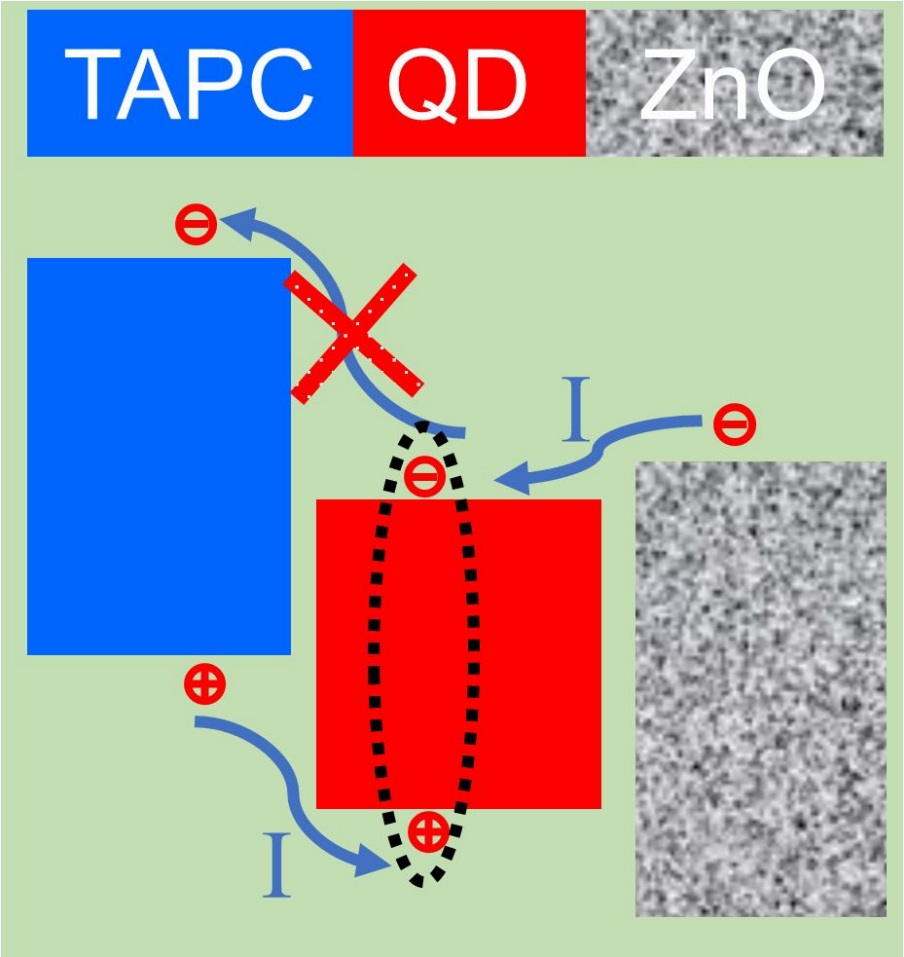

Figure S10 Schematic diagrams of the working mechanism for TAPC based device. **I** represents the charge injection from charge transport layers to the QDs, **II** refers to as the electron leakage, and **III** is the ET process.

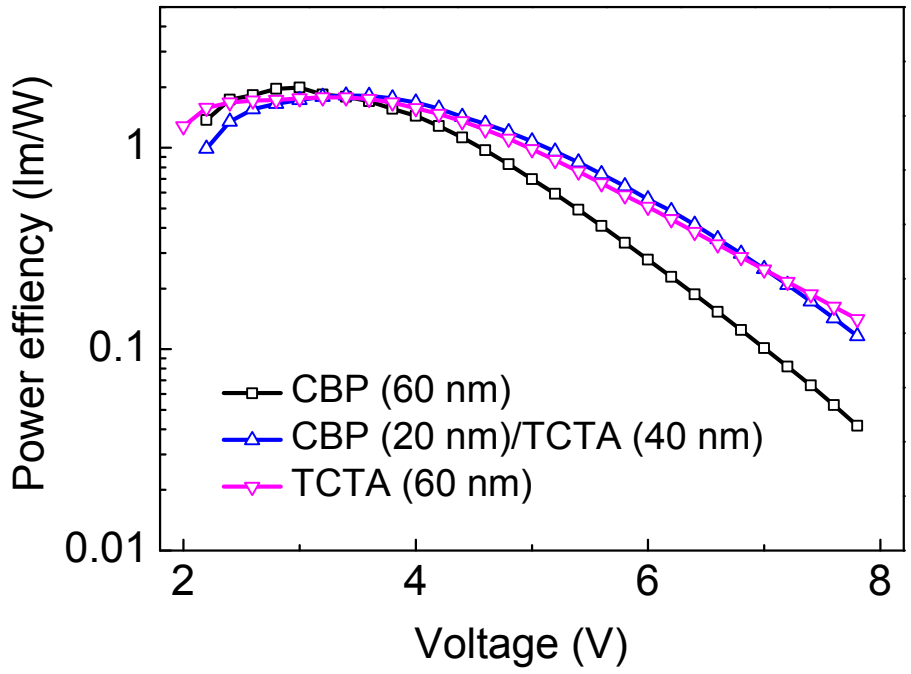

Figure S11 Power efficiency-voltage curves of devices based different HTLs

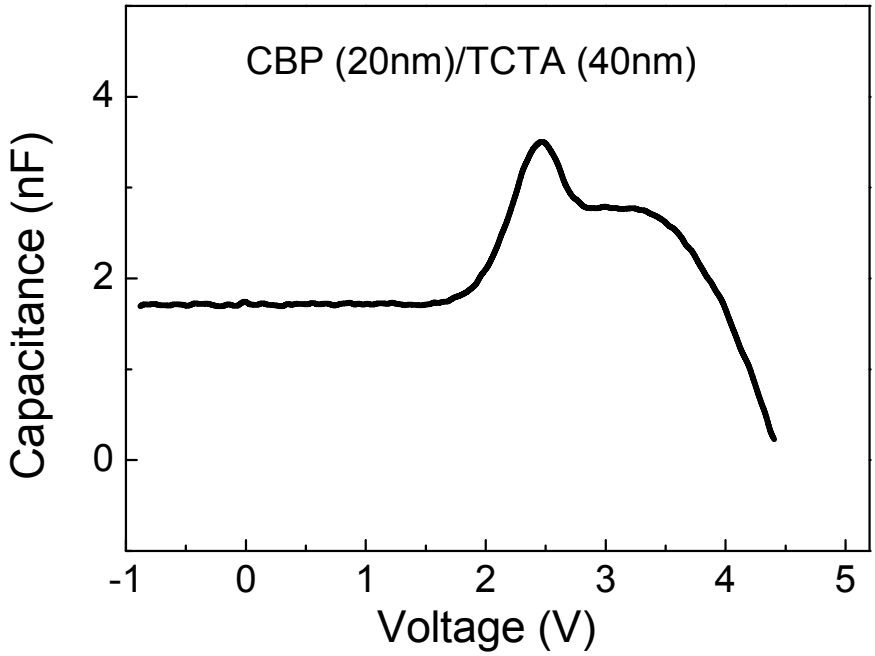

Figure S12 Capacitance versus driving voltages for bi-layer HTL device.

Reference

(1). Jara, D. H.; Stamplecoskie, K. G.; Kamat, P. V. Two Distinct Transitions in Cu_xInS_2 Quantum Dots. Bandgap Versus Sub-Bandgap Excitations in Copper-Deficient Structures. *J. Phys. Chem. Lett.* **2016**, *7* (8), 1452-1459.

(2). Jara, D. H.; Yoon, S. J.; Stamplecoskie, K. G.; Kamat, P. V. Size-Dependent Photovoltaic Performance of Cuins2 Quantum Dot-Sensitized Solar Cells. *Chem. Mater.* **2014**, *26* (24), 7221-7228.

(3). Nowy, S.; Ren, W.; Elschner, A.; Lovenich, W.; Brutting, W. Impedance Spectroscopy as a Probe for the Degradation of Organic Light-Emitting Diodes. *J. Appl. Phys.* **2010**, *107* (5), 054501.

(4). Ji, W. Y.; Liu, S. H.; Zhang, H.; Wang, R.; Xie, W. F.; Zhang, H. Z. Ultrasonic Spray Processed, Highly Efficient All-Inorganic Quantum-Dot Light-Emitting Diodes. *ACS Photonics* **2017**, *4* (5), 1271-1278.